THE IMPEDANCE OF SODIUM–SULPHUR CELLS AT VERY LOW FREQUENCIES

P. J. JOHNSON

Chloride Silent Power Ltd., Davy Road, Astmoor, Runcorn WA7 1PZ, Cheshire (U.K.)

(Received February 6, 1989; in revised form December 6, 1989)

Summary

The impedance of sodium–sulphur cells as a function of state of charge has been measured in the frequency range 10^{-5} - 10^{3} Hz. The impedance spectra of cells near the top of charge show a depressed semi-circle in the complex plane. As the single phase region is approached the impedance exhibits Warburg behaviour below 10 mHz, and below 0.4 mHz the impedance rises sharply. The rise in impedance at low frequencies is attributed to concentration polarisation of the sulphur electrode, which arises when the electrochemical reaction rate is controlled by the diffusion rate of sodium ions through the polysulphide electrode. This behaviour is analysed in terms of an equivalent circuit, and the significance of the resulting values for the parameters of the circuit is discussed.

Introduction

The high power and energy densities of the sodium–sulphur battery have led to it being considered for a wide variety of applications, for example, utility load levelling, automotive traction and satellite. Each of these applications imposes a unique set of performance requirements upon the battery, and these requirements influence the capacity, power output and cycling conditions of the constituent cells. The performance of these cells is in turn strongly affected by their internal resistance and its stability both within each charge–discharge cycle and throughout the projected lifetime of the cell [1]. The internal resistance of the cell also determines the rate of heat generation within the cell. Details of the internal resistance of a cell as a function of charge state are therefore essential for the design of a thermal management system for a battery. The frequency dependence of cell impedance, particularly at frequencies of the same order of magnitude as the intended application may impose, is also important. These frequencies may be very low, for example an electric vehicle which is operating in an urban environment and is equipped with regenerative braking driving may subject the battery to charge–discharge cycles of many minutes duration

0378-7753/90/$3.50

[2]. A relatively high internal resistance is particularly detrimental as it limits the energy efficiency of cells and reduces the specific peak power of the battery.

Previous studies of cell impedance have primarily concentrated on elucidating the mechanisms of cell operation, and, in particular, diagnosing the cause of poor cell performance [3 - 5]. These measurements have concentrated on higher frequencies, although recently McKubre *et al.* [6] have extended these measurements into the millihertz region. To enable predictions of vehicle performance, where duty cycles of the order of many hours may be encountered, data extending into the microhertz frequency domain are desirable. This paper reports impedance measurements over the range of frequencies that are likely to be encountered by a battery in service.

Experimental

The sodium–sulphur cells used in these experiments were constructed in our laboratories and were tubular central sodium cells of 15 A h capacity, the principle features of which have been described previously [7]. The sulphur electrode was constructed using carbon fibres (Union Carbide Thornel VMA) orientated perpendicularly to the solid electrolyte and a barrier layer next to the electrolyte of alumina fibres to form a dual-mat-type electrode. The cells were warmed to 350 °C and were subject to at least forty charge–discharge cycles (charge: 90 mA cm^{-2} and discharge: 130 mA cm^{-2}) prior to making a.c. measurements, and were maintained at this temperature (±0.5 °C) while measurements were being taken.

The temperature of each cell was measured using two chromel–alumel thermocouples, the sensing ends of which were placed one on each of the electrode terminals. The two alumel leads also served as voltage probes to the cell.

Impedance measurements were carried out using a Solartron model 1250 frequency response analyser coupled to a Solartron model 1286 electrochemical interface operating in potentiostatic mode. Frequencies were swept from 1000 Hz logarithmically downwards, taking thirty measurements per decade. If no dispersion tail had been detected by 1 mHz then the sweep was terminated to reduce the experimental time, although in some cases measurements were extended to frequencies as low as 3×10^{-5} Hz (in this case taking seven measurements per decade). A 10 Hz low-pass filter was also incorporated into the measuring circuit to reduce interference from the mains-powered furnace when measuring below 1 Hz.

The cells were progressively discharged in one ampère-hour steps. An equilibration period of at least ten hours was allowed prior to each measurement.

Results and discussion

The impedance spectra for the 15 A h cell are shown as Nyquist plots in Fig. 1 for various depths of discharge. Measurements taken at depths of discharge which correspond to the two-phase region of operation of the sulphur electrode show only a depressed semi-circular arc in the complex plane (plots D and E). As the sulphur electrode enters the single phase region a Warburg tail appears at frequencies below 10 mHz, and the cell impedance rises as the frequency is further reduced (plots A, B and C).

The impedance behaviour shown in Fig. 1 can be interpreted in terms of an equivalent circuit model of the type shown in Fig. 2. In this model, the ohmic resistance represents the resistance of the electronically conducting components of the cell (*i.e.*, the cell case, the sodium electrode and the carbon fibres) and the solid electrolyte. Although Armstrong *et al.* [8] showed that the sodium/electrolyte interface can result in a frequency dispersion, it occurs at a frequency outside the range of the present work, and consequently an ohmic model of this interface is adequate.

The analysis of a single depressed semi-circular arc in the complex plane has been described in detail by Macdonald and Johnson [9]. This analysis allows an impedance arc to be fully characterised in terms of four parameters: R_∞, the high frequency intercept with the real axis; R_p, the chord length of the arc on the real axis; θ, the angle by which the semi-circle is depressed below the real axis; τ_R, the characteristic time for the arc ($\tau_R = 1/\omega_0$, where ω_0 is the angular frequency at the maximum of the

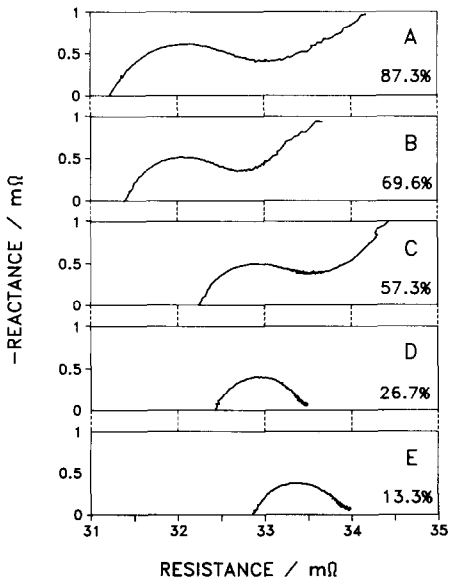

Fig. 1. Nyquist plots for the cell at five discharge states. (The depth of discharge is shown as a percentage of cell capacity measured to 1.76 V.)

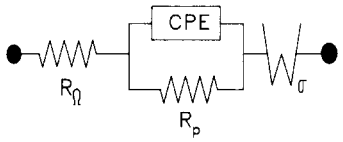

Fig. 2. An equivalent circuit model for a sodium–sulphur cell where R_p = polarisation resistance, W_σ = Warburg impedance, R_Ω = ohmic resistance, *CPE* = constant phase element.

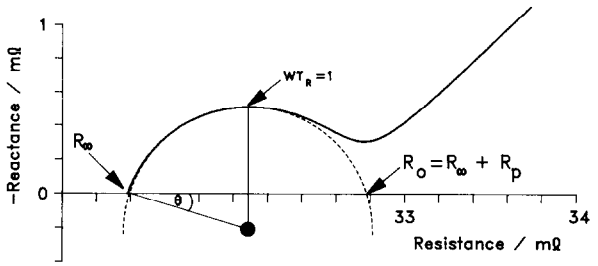

Fig. 3. The parameters derived from a Nyquist plot used in the analysis of impedance data.

arc). Figure 3 illustrates how these parameters are extracted from a Nyquist plot. Note that even if the arc is distorted by a Warburg tail, a semi-circle may still be fitted to the high frequency points, as shown in the Figure. The depression of the semi-circle arises when there is a distribution of relaxation times, which may occur, for example, if an interfacial or bulk process is controlled by a distribution of activation energies. Such a process is modelled in the equivalent circuit by a distributed impedance element such as the constant phase element (CPE). The impedance of this element is given by $Z_{CPE} = 1/A_0(j\omega)^\psi$ [10]. In the limits $\psi = 0$, A_0 reduces to $1/R$, a conductance, and when $\psi = 1$, A_0 is equal to C, a capacitance. The fractional exponent ψ is related to the angle θ by the simple relationship $\psi = 1 - 2\theta/\pi$.

The high frequency intercept with the real axis yields the ohmic component of cell resistance. The variation of ohmic resistance of the cell with depth of discharge is shown in Fig. 4. This term clearly decreases with increasing depth of discharge. This may be attributed to the higher conductivity of the lower polysulphides [11].

It is interesting to note that the chord length of the arc increases as the cell is progressively discharged. This increase is non-linear, the resistance rising sharply as the end of discharge is approached, as can be seen in Fig. 5. As both the ohmic and polarisation resistances vary with depth of discharge the Nyquist plot will be distorted if the cell is not at equilibrium. The fitting of a semi-circle will be increasingly difficult and the derived parameters more inaccurate the more distorted the plot becomes. The observed scatter in the resistance plots therefore may be due to the cells still being polarised when the measurements were taken.

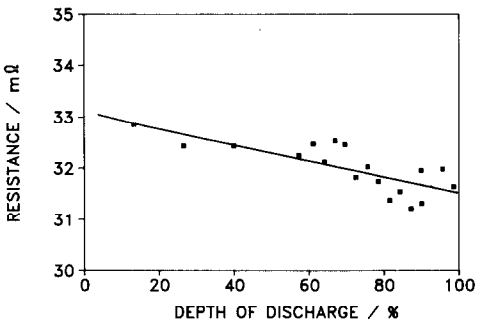

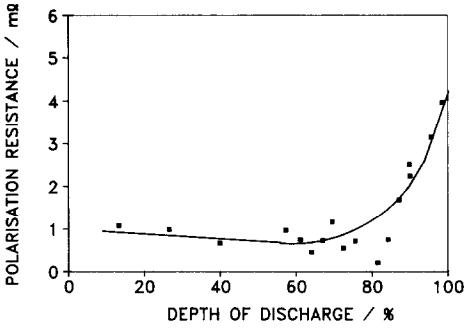

Fig. 4. The ohmic component of cell resistance as a function of depth of discharge.

Fig. 5. The variation of polarisation resistance with depth of discharge.

The two other parameters which may be inferred from the Nyquist plot are θ and τ_R. Within the limits of precision of the experiment these two parameters were found to be invariant with respect to depth of discharge. The values obtained for these parameters are $\theta = 18 \pm 2°$ and $\tau_R = 1.9 \pm 0.2 \times 10^{-2}$ s.

The Warburg term is not directly obtainable from the Nyquist plot. This impedance is related to angular frequency by the expression

$$Z_w = \sigma\omega^{-1/2} - j\sigma\omega^{-1/2} \quad (1)$$

where σ is the Warburg coefficient, which for a single diffusing species is given by [9]

$$\sigma = RT/n^2F^2C(2D)^{1/2} \quad (2)$$

where C and D are the concentration and diffusion coefficient of the diffusing species, respectively. The experimental value of the coefficient is inferred from the slope of a plot of the imaginary component of impedance against $\omega^{-1/2}$. The variation of Warburg coefficient with depth of discharge is shown in Fig. 6. The non-zero value for the Warburg coefficient when the cell is operating in the two-phase region is at first sight surprising, simply

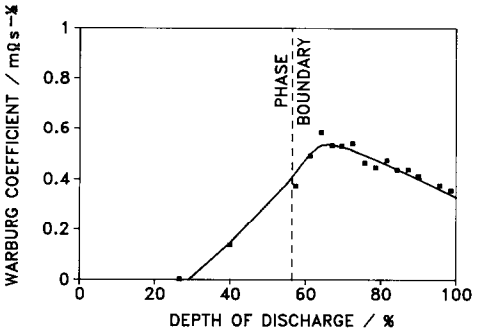

Fig. 6. The variation of Warburg coefficient with depth of discharge.

because there are two immiscible phases present and, consequently, no concentration gradients to allow diffusion to control the reaction. The cell under load is not under equilibrium conditions, however, and the electrode structure is designed to maintain a high concentration of polysulphide species close to the electrolyte surface. Two reactions are therefore possible, either direct reaction of the sodium ions with sulphur, or the further reduction of polysulphide (which subsequently reacts with any remaining sulphur). Only the latter reaction is diffusion controlled. Thus, as the amount of available sulphur decreases, then the latter reaction begins to dominate. The Warburg coefficient, therefore, will increase as the area over which the polarisable reaction is occurring increases. In the single-phase region the Warburg coefficient, as measured for the cell, will be dependent on the diffusion coefficients and concentrations of the ionic species of the sulphur electrode. The maximum in the observed curve occurs at about 65% discharged, which corresponds closely to the composition $Na_2S_{4.7}$. Cleaver [12] has reported a maximum in the viscosity for sodium polysulphides at this composition.

Consider the cell when it is 60% discharged, *i.e.*, when the polysulphide composition corresponds to the empirical formula Na_2S_5. The density of this melt at 350 °C is 1.75 g cm^{-3} [13], giving a sodium ion concentration of 17 M. Using this value along with the value for the interdiffusion coefficient of sodium pentasulphide (as reported by Divisek *et al.* [14]) of 1.6×10^{-6} cm^{-2} s^{-1}, and substituting in eqn. (2), gives a calculated value for the area specific Warburg coefficient of $\sigma_{calc} = 16.3$ mΩ cm^2 $s^{-1/2}$. Comparing this value with the observed value for the cell as a whole at this state of charge of 0.5 mΩ $s^{-1/2}$ implies an active electrode area of 32.6 cm^2. Even if the values of the parameters used in eqn. (2) were in error by up to an order of magnitude, it is inconceivable that the Warburg term arises as a result of a diffusion process within the bulk of the sulphur electrode. A more probable origin is the high resistance barrier layer between the solid electrolyte and the ends of the carbon fibres of the sulphur electrode. The area of this barrier layer was determined to be 30.4 cm^2, a value which is in reasonable agreement with the calculated active area, given the uncertainty of the experimental parameters used in eqn. (2). This result verifies the model developed by McKubre *et al.* [6b], which assumed that the edge of the carbon fibre electrode would behave electrochemically as a smooth planar electrode of orientation parallel to the solid electrolyte surface. The incorporation of a Warburg term with an impedance described by eqn. (1) into the equivalent circuit model will adequately describe this behaviour.

The Nyquist plot for the cell at 95% discharge, where the frequency measurements have been extended down to 30 μHz, is shown in Fig. 7. At frequencies below 0.4 mHz the slope of this curve increases sharply. The observed deviation, at very low frequencies, from pure Warburg behaviour suggests that the assumption of a semi-infinite transmission line composed of only resistors and capacitors is no longer valid at frequencies

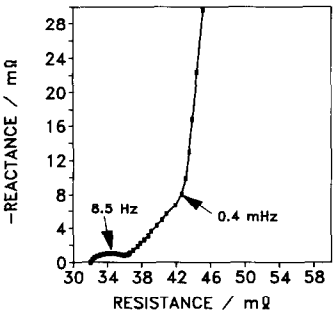

Fig. 7. Nyquist plot for the cell at 95% discharge.

below 0.4 mHz. At lower frequencies the total charge passed in each half cycle becomes sufficient to affect significantly the state of charge of the cell. Thus, in the single-phase region, on the charging half-wave the equilibrium cell potential will rise and on the discharging half-wave the equilibrium cell potential will fall. The net result is that the overpotential falls with decreasing frequency even though the applied potential is held constant. Under these circumstances the cell potential follows or 'tracks' the applied potential. The cell therefore behaves as an electrolytic capacitor, which explains the observed increase in slope of the curve in the Nyquist plot, and the frequency of 0.4 mHz represents the lower limit below which the assumption of semi-infinite behaviour is no longer valid.

The phenomenon of concentration polarisation in sodium–sulphur cells may now be analysed in terms of a smooth, planar sulphur electrode. As the cell is discharged into the single-phase region the polysulphide at the edge of the carbon fibres will be reduced to a lower species, and so a concentration gradient will be established across the barrier layer. The polysulphides in the barrier layer will thus become relatively sulphur-rich near the solid electrolyte and sodium-rich near the edge of the carbon fibres. The transference number of polysulphide ions in a melt of uniform composition has been shown by Risch and Newman [15] to be small, indicating that the mobility of the sodium ions is considerably greater than the polysulphide ions. This result was not unexpected since the relative ion sizes are so different. At first it would appear, therefore, that the diffusion of polysulphide ions is the rate determining step in the decay of concentration gradients. However, Divisek *et al.* [14] have also measured the self-diffusion coffficient of sulphur in polysulphide using a tracer technique, and found it to be more than an order of magnitude greater than the interdiffusion coefficient. They explained their results by proposing two transport mechanisms: in the first case, a polysulphide ion and simultaneously a sodium ion are diffusing relative to each other, *i.e.*, the complete polysulphide ion is mobile, whereas in the second case the transport of an uncharged sulphur species takes place by a rapid exchange of sulphur atoms from one polysulphide species to another without being strongly bound to the ionic structure. In this way the mass transport of sulphur

is relatively rapid and so it is the interdiffusion process which is the rate determining step that gives rise to the observed Warburg behaviour in sodium–sulphur cells.

This analysis of the impedance results shows only a slight increase in polarisation resistance when the cell is deeply discharged (>80%) and this is partly offset by a decrease in ohmic resistance. The cell impedance in the single phase region is therefore dominated by the Warburg term. As a consequence of the frequency dependency of this term, the internal heating of the battery will depend not only upon the state of charge of the battery but also on the length of the duty cycles to which it is subjected. The thermal management system for a battery must be designed to accommodate this frequency dependent rate of heat generation. The four element equivalent circuit model for the sodium–sulphur cell proposed in this work allows linear circuit analysis techniques to be used in the mathematical modelling of batteries.

Acknowledgement

This research work was partly supported by the U.S. Department of Energy Office of Energy Storage through Sandia National Laboratories, contract number 48-8837.

References

1 A. A. Koenig, *Proc. 33rd Int. Power Sources Symp., Cherry Hill, NJ, U.S.A., 1988*, p. 555.
2 E. J. Dowgiallo and R. J. Kevala, *Proc. 8th Int. Electric Vehicle Symp., Washington, DC, U.S.A., 1986*, p. 166.
3 B. R. Karas, *J. Electrochem. Soc., 132* (1985) 1261.
4 B. R. Karas and R. N. King, *J. Electrochem. Soc., 132* (1985) 1266.
5 G. Staikov, P. D. Yankulov, B. S. Savova-Stoynov and Z. B. Stoynov, *J. Appl. Electrochem., 15* (1985) 895.
6 (a) M. C. M. McKubre, S. I. Smedley and F. L. Tanzella, *Proc. Symp. NaS Batteries, 170th Electrochemical Society Meet., San Diego, CA, U.S.A., 1987*, p. 214; (b) *J. Electrochem. Soc., 136* (1989) 1969.
7 I. W. Jones, *Proc. DOE/EPRI Beta Battery Workshop VII, EPRI AP-6012-SR*, EPRI, Palo Alto, CA, U.S.A., 1988, p. 13-1.
8 R. D. Armstrong, T. Dickinson and J. Turner, *J. Electroanal. Chem. Int. Electrochem., 44* (1973) 157.
9 J. R. Macdonald and W. B. Johnson, in J. R. Macdonald (ed.), *Impedance Spectroscopy*, Wiley, New York, 1987.
10 J. R. Macdonald, *Solid State Ionics, 13* (1984) 147.
11 B. Cleaver, A. J. Davies and M. D. Hames, *Electrochim. Acta, 18* (1973) 719.
12 B. Cleaver, in R. P. Tischer (ed.), *The Sulphur Electrode*, Academic Press, New York, 1983.
13 D.-G. Oei, *Inorg. Chem., 12* (1973) 438.
14 J. Divisek, F. G. Bodewig, J. Mergel, H. Lippert and B. Kastening, *J. Electrochem. Soc., 127* (1980) 357.
15 T. Risch and J. Newman, *J. Electrochem. Soc., 135* (1988) 1715.